Control of a continuously variable transmission in an experimental vehicle

Document Version:
Accepted manuscript including changes made at the peer-review stage

Please check the document version of this publication:

• A submitted manuscript is the version of the article upon submission and before peer-review. There can be important differences between the submitted version and the official published version of record. People interested in the research are advised to contact the author for the final version of the publication, or visit the DOI to the publisher's website.
• The final author version and the galley proof are versions of the publication after peer review.
• The final published version features the final layout of the paper including the volume, issue and page numbers.

[Link to publication](#)

CONTROL OF A CONTINUOUSLY VARIABLE TRANSMISSION IN AN EXPERIMENTAL VEHICLE

Michiel Pesgens [*] **Bas Vroemen** [**,1]
Frans Veldpaus [*] **and Maarten Steinbuch** [*]

*[*] Technische Universiteit Eindhoven,
P.O. Box 513, 5600 M.B. Eindhoven, The Netherlands
[**] Drivetrain Innovations b.v.,
Horsten 1, 5612 AX, The Netherlands*

Abstract: This paper focusses on the development of a component controller for a hydraulically actuated metal push-belt Continuously Variable Transmission (CVT), using models for the mechanical and the hydraulic part of the CVT. The ratio controller guarantees that one clamping pressure setpoint is minimal, while the other is raised above the minimum level to enable shifting. This approach is beneficial with respect to efficiency and wear. Vehicle experiments show that good tracking is obtained. The largest deviations from the ratio setpoint are caused by hardware limitations. *Copyright © 2003 IFAC*

Keywords: Continuously variable transmission, Feedforward compensation, Feedback linearization, Hydraulic actuators, Constraints

1. INTRODUCTION

The application of a Continuously Variable Transmission (CVT) instead of a stepped transmission is not new. Already in the fifties Van Doorne introduced a rubber V-belt CVT for vehicular drivelines. Modern, electronically controlled CVTs make it possible to operate the combustion engine for any vehicle speed in a wide range of operating points, for instance in the fuel optimal point. For this reason, CVTs get increasingly important in hybrid vehicles, see *e.g.,* Frank and Francisco (2002), Ozeki and Umeyama (2002) and Vroemen (2001). Accurate control of the CVT transmission ratio is essential to achieve the intended fuel economy and moreover ensure good driveability.

The ratio setpoint is generated by the hierarchical (coordinated) controller of Fig. 1. This controller uses the accelerator pedal position as the input and generates setpoints for the local controllers of the throttle and of the CVT.

The CVT and its hydraulic actuation system is depicted in Fig. 2. The hydraulic system not only has to guarantee good tracking behavior of the CVT but also has to realize clamping forces that, on the one hand, are high enough to prevent belt slip but, on the other hand, are as low as possible to maximize the transmission efficiency and to reduce wear. The main focus of this paper is on the ratio control of the CVT, using the hydraulic actuation system of Fig. 2. The presented control concept is based on the work of Stouten (2000) and Vroemen (2001). It enables tracking of the ratio setpoint, with at least one of the two pulley pressures equal to its lower constraint. Even though the controller effectively changes from controlling one of the

[1] E-mail corresponding author:
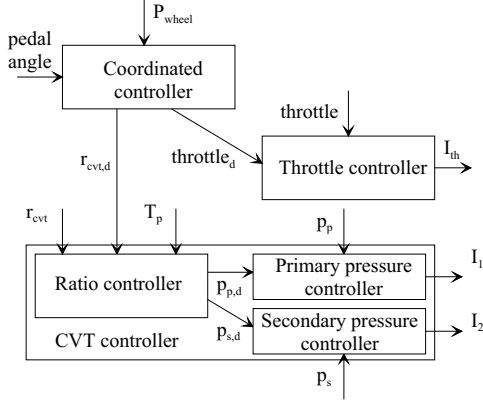vroemen@dtinnovations.nl
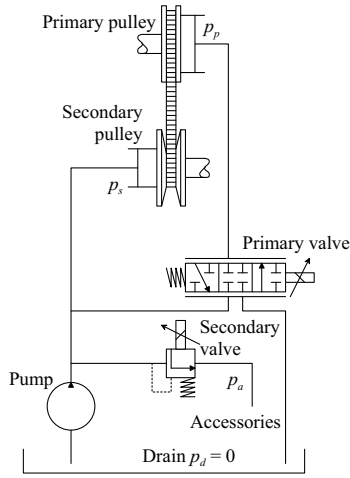
Fig. 1. Hierarchical powertrain control

Fig. 2. Variator with hydraulic system

two pressures to the other, no actual switching between different controllers takes place. Among the approaches seen in literature, some incorporate a switching algorithm (Spijker, 1994; Vroemen, 2001), whereas others control only one of the two pressures (van der Laan and Luh, 1999; Vanvuchelen, 1997). While the former approach cannot guarantee one of the two pressures to be equal to its lower constraint, the latter cannot explicitly prevent the uncontrolled pressure to stay above its lower constraint.

The remainder of this paper is organized as follows. First, a mathematical model is derived for the mechanical part of the CVT in Section 2. Next, in Section 3, the hydraulic part is modelled. The physical constraints, imposed by the hydraulic system, are discussed in Section 4. These constraints are taken into account by the CVT ratio controller, that is developed in Section 5 and is based on the earlier derived models for the mechanical and the hydraulic CVT parts. The tracking performance of this controller is experimentally evaluated in Section 6. Finally, Section 7 gives some concluding remarks.

2. THE PUSHBELT CVT

The CVT (Fig. 3) considered here is equipped with a Van Doorne metal pushbelt. This belt consists of a large number (around 350) of V-shaped steel block elements, held together by a number (between 9 and 12) of thin steel tension rings. The belt runs on the primary pulley at the engine side and the secondary pulley at the wheel side. Each pulley consists of one axially fixed and one moveable sheave, operated by means of a hydraulic cylinder. The cylinders can be pressurized, generating axial clamping forces or thrusts on the belt, necessary for transmission of torque without macro-slip of the belt and for ratio change.
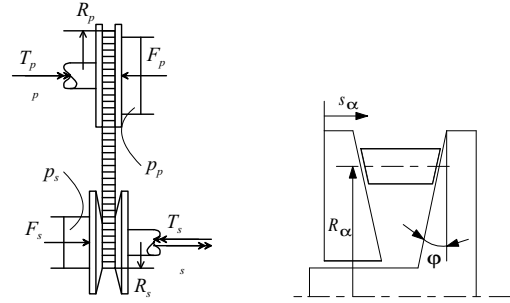

Fig. 3. Variator and pulley sheave definitions

The variator transmission ratio $r_{cvt} \in [r_{cvt,LOW}, r_{cvt,OD}]$ is defined as the ratio of secondary pulley speed ω_s over primary pulley speed ω_p, so:

$$r_{cvt} = \frac{\omega_s}{\omega_p} \qquad (1)$$

The following assumptions have been made:

- the pulleys are rigid and perfectly aligned
- the V-shaped blocks are rigid and the steel rings are inextensible
- the power transmission between the belt and the pulleys is based on Coulomb friction
- the clamping forces are large enough to prevent belt slip

Using these assumptions, the running radii R_p and R_s on the primary and secondary pulley are functions of the ratio r_{cvt} only and are related by:

$$R_p = r_{cvt} \cdot R_s \qquad (2)$$

The axial position s_α (α=p for the primary pulley, α=s for the secondary one) of the moveable pulley sheave of pulley α is also completely determined by r_{cvt}.

Denoting the taper angle of the conical sheaves by φ (see Fig. 3) it is seen that:

$$s_\alpha = 2 \cdot \tan(\varphi) \cdot (R_\alpha - R_{\alpha,min}) \qquad (3)$$

Subscript "max" (or "min") implies the maximum (or minimum) value possible, unless stated otherwise. Differentiation with respect to time yields

the axial velocity $\dot{s}_\alpha$ of the moveable sheave of pulley α:

$$\dot{s}_\alpha = \nu_\alpha(r_{\mathrm{cvt}}) \cdot \dot{r}_{\mathrm{cvt}} \qquad (4)$$

where the function ν_α follows from the geometry of the variator.

The critical pulley clamping force (equal for both pulleys, neglecting power losses in the variator's) is given by:

$$F_{\mathrm{crit}} = \frac{\cos(\varphi) \cdot |T_{\mathrm{p}}|}{2 \cdot \mu \cdot R_{\mathrm{p}}} \qquad (5)$$

where μ is the friction coefficient between pulley and belt and T_p is the primary pulley torque. The torque ratio τ_α is the ratio of transmitted torque and maximally transmittable torque without belt slip for pulley α:

$$\tau_\alpha = \frac{T_\alpha}{T_{\alpha,\mathrm{max}}} \qquad (6)$$

An important part of the model for the mechanical part of the CVT is the submodel for the rate of ratio change as a function of, for instance, the clamping forces. Submodels of this type are proposed, amongst others, by Guebeli *et al.* (1993), Ide *et al.* (1994), Ide *et al.* (1996) and Shafai *et al.* (1995). The blackbox model of Ide is preferred here since it reasonably describes the results of a series of experiments with metal V-belt CVTs (Stouten, 2000; Vroemen, 2001).

The steady state version of Ide's model yields a relation for the primary clamping force F_{p} that is required to maintain a given ratio r_{cvt} with a given secondary clamping force F_{s} and a given primary torque T_{p}.

$$F_{\mathrm{p}} = \kappa(r_{\mathrm{cvt}}, \tau) \cdot F_{\mathrm{s}} \qquad (7)$$

Here, a dimensionless modified torque ratio τ similar to Eq. (6) is introduced, depending only on measurable variables. The quantity κ in Eq. (7), the thrust ratio, depends in a very nonlinear way on the CVT ratio r_{cvt} and the torque ratio τ.

For instationary situations, Ide's model states that the rate of ratio change $\dot{r}_{\mathrm{cvt}}$ is a function of the ratio r_{cvt}, primary pulley speed ω_{p}, clamping forces F_{p} and F_{s} and torque ratio τ:

$$\begin{aligned} \dot{r}_{\mathrm{cvt}} &= k_r(r_{\mathrm{cvt}}) \cdot |\omega_{\mathrm{p}}| \cdot F_{\mathrm{shift}}; \\ F_{\mathrm{shift}} &= F_p - \kappa(r_{\mathrm{cvt}}, \tau) \cdot F_{\mathrm{s}} \end{aligned} \qquad (8)$$

The axial force difference F_{shift} is called the shift force. k_r is a nonlinear function of the ratio r_{cvt} only. Both k_r and κ have been obtained experimentally.

The occurrence of ω_{p} in Eq. (8) is plausible because an increasing shift force is needed for decreasing pulley speeds to obtain the same rate of ratio change. The reason is that less V-shaped blocks enter the pulleys per second when the pulley speed decreases. As a result the radial belt
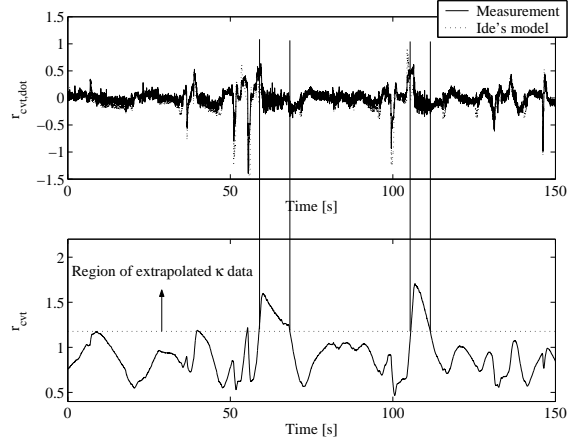

Fig. 4. Comparison of shifting speed, Ide's model vs. measurement

travel per revolution of the pulleys must increase and this requires a higher shift force. However, it is far from obvious that the rate of ratio change is *proportional* to both the shift force and the primary pulley speed.

To validate Ide's model, the shifting speed $\dot{r}_{\mathrm{cvt}}$, recorded during a road experiment, is compared with the same signal predicted by the model. Model inputs are the hydraulic pulley pressures (p_{p},p_{s}) and pulley speeds (ω_{p},ω_{s}) together with the estimated primary pulley torque ($\hat{T}_{\mathrm{p}}$). The result is depicted in Fig. 4. The model describes the shifting speed well, but for some upshifts it predicts too large values. This happens only for high cvt ratios, *i.e.*, $r_{\mathrm{cvt}} > 1.2$, where the data of κ is unreliable due to extrapolation.

3. THE HYDRAULIC SYSTEM

The hydraulic part of the CVT (see Fig. 2) essentially consists of a roller vane pump (directly connected to the engine shaft), two solenoid valves and a pressure cylinder on each of the moveable pulley sheaves. The volume between the pump and the two valves including the secondary pulley cylinder is referred to as the secondary circuit, the volume directly connected to and plus the primary pulley cylinder is the primary circuit. Excessive flow in the secondary circuit bleeds off towards the accessories, whereas the primary circuit can blow off towards the drain. Pressures are defined relative to the atmospheric drain pressure p_{d}.

As the model will only be used to determine the hydraulic system constraints needed for the feedforward control, the following assumptions have been made:

- the compressibility of the oil is neglected
- the oil temperature is constant
- all leakage flows are negligible

The clamping forces F_p and F_s are realized mainly by the hydraulic cylinders on the moveable sheaves. Since the cylinders are an integral part of the pulleys, they rotate with an often very high speed, so centrifugal effects have to be taken into account and the pressure in the cylinders will not be homogeneous. Therefore, the clamping forces will also depend on the pulley speeds ω_p and ω_s. Furthermore, a pre-stressed linear elastic spring with stiffness k_{spr} is attached to the moveable secondary sheave. This spring has to guarantee a minimal clamping force when the hydraulic system fails. Together this results in the following relations for the clamping forces:

$$F_p = A_p \cdot p_p + c_p \cdot \omega_p^2 \qquad (9)$$

$$F_s = A_s \cdot p_s + c_s \cdot \omega_s^2 + k_{spr} \cdot s_s + F_0 \qquad (10)$$

where c_p and c_s are constants and F_0 is the force in the spring if the secondary moveable sheave is at position $s_s = 0$. Furthermore, A_p and A_s are the pressurized piston surfaces. In the hydraulic system of Fig. 2 the primary pressure is smaller than the secondary pressure if there is an oil flow from the secondary to the primary circuit. Therefore, to guarantee that in any case the primary clamping force can be up to twice as large as the secondary clamping force, the primary piston surface A_p is approximately twice as large as the secondary surface A_s.

The law of mass conservation, applied to the primary circuit, results in:

$$Q_{sp} = Q_{pd} + Q_{p,V} \qquad (11)$$

Q_{sp} is the oil flow from the secondary to the primary circuit, Q_{pd} is the oil flow from the primary circuit to the drain, and $Q_{p,V}$ is the flow, needed for pulley cylinder displacement. The oil flow Q_{sp} is given by:

$$Q_{sp} = c_f \cdot A_{sp}(x_p) \cdot \sqrt{\frac{2}{\rho} \cdot |p_s - p_p|} \cdot \text{sign}(p_s - p_p) \qquad (12)$$

where c_f is a constant flow coefficient and ρ is the oil density. The equivalent valve opening area A_{sp} depends on the primary valve stem position x_p. Flow Q_{pd} follows from:

$$Q_{pd} = c_f \cdot A_{pd}(x_p) \cdot \sqrt{\frac{2}{\rho} \cdot p_p} \qquad (13)$$

Here, A_{pd} is the equivalent opening area of the primary valve for the flow from primary circuit to the drain. The construction of the valve implies that $A_{sp}(x_p) \cdot A_{pd}(x_p) = 0$ for all possible x_p. The flow due to a change of pulley cylinder volume is described by:

$$Q_{\alpha,V} = A_\alpha \cdot \dot{s}_\alpha \qquad (14)$$

with $\dot{s}_\alpha$ given by Eq. (4).

Application of the law of mass conservation to the secondary circuit yields

$$Q_{pump} = Q_{sp} + Q_{sa} + Q_{s,V} \qquad (15)$$

The flow Q_{pump}, generated by the roller vane pump, depends on the pressure p_s at the pump outlet, on the angular speed ω_e of the engine shaft and on the pump mode m ($m = $ SS for single sided and $m = $ DS for double sided mode), so $Q_{pump} = Q_{pump}(\omega_e, p_s, m)$. Q_{sa} is the flow from the secondary circuit to the accessories. Flow Q_{sa} is modelled as:

$$Q_{sa} = c_f \cdot A_{sa}(x_s) \cdot \sqrt{\frac{2}{\rho} \cdot |p_s - p_a|} \cdot \text{sign}(p_s - p_a) \qquad (16)$$

where the equivalent valve opening A_{sa} of the secondary valve depends on the valve stem position x_s.

Now that a complete model of the pushbelt CVT and its hydraulics is available, the controller and its operational constraints can be derived.

4. THE CONSTRAINTS

The CVT ratio controller in fact controls the primary and secondary pressure. Several pressure constraints have to be taken into account by this controller:

(1) the torque constraints $p_\alpha \geq p_{\alpha,torque}$ to prevent slip on the pulleys;
(2) the lower pressure constraints $p_\alpha \geq p_{\alpha,low}$ to keep both circuit filled with oil. Here, fairly arbitrary, $p_{p,low} = 3$ [bar] is chosen. To enable a sufficient oil flow Q_{sa} to the accessory circuit, and for a proper operation of the passive valves in this circuit it is necessary that Q_{sa} is greater than a minimum flow $Q_{sa,min}$. A minimum pressure $p_{s,low}$ of 4 [bar] turns out to be sufficient;
(3) the upper pressure constraints $p_p \leq p_{p,max}$ and $p_s \leq p_{s,max}$, to prevent damage to the hydraulic lines, cylinders and pistons. Hence, $p_{p,max} = 25$ [bar], $p_{s,max} = 50$ [bar].
(4) the hydraulic constraints $p_\alpha \geq p_{\alpha,hyd}$ to guarantee that the primary circuit can bleed off fast enough towards the drain and that the secondary circuit can supply sufficient flow towards the primary circuit.

The pressures $p_{p,torque}$ and $p_{s,torque}$ depend on the critical clamping force F_{crit}, Eq. (5). A safety factor k_s has been introduced to account for disturbances on the estimated torque $\hat{T}_p$, such as shock loads at the wheels. Then, the pulley clamping force (equal for both pulleys, neglecting the variator efficiency) needed for torque transmission becomes:

$$F_{torque} = \frac{\cos(\varphi) \cdot (|\hat{T}_p| + k_s \cdot \hat{T}_{p,max})}{2 \cdot \mu \cdot R_p} \qquad (17)$$

Consequently, the resulting pressures can be easily derived using Eq.s (9) and (10).

Constraints (4) are based on the law of mass conservation for the primary circuit. It is mentioned again that the flows Q_{sp} and Q_{pd} can never be unequal to zero at the same time. In the sequel, it is chosen to replace the rate of ratio change $\dot{r}_{cvt}$ by the desired rate of ratio shift $\dot{r}_{cvt,d}$. If $\dot{r}_{cvt,d} < 0$ then oil has to flow out of the primary cylinder to the drain, so $Q_{pd} > 0$ and $Q_{sp} = 0$ holds for Eq. (11). The pressure $p_{p,hyd}$ can now be easily derived using Eq.s (14) and (13), using the maximum primary valve opening $A_{pd,max}$ to the drain.

In a similar way, a relation for the pressure $p_{s,hyd}$ can be derived. This constraint is especially relevant if $\dot{r}_{cvt} > 0$, *i.e.*, if Q_{sp} has to be positive and, as a consequence, $Q_{pd} = 0$. Again, using Eq. (11), pressure $p_{s,hyd}$ can be derived with Eq.s (14) and (12), using the maximum primary valve opening $A_{pd,max}$ from the secondary to the primary oil circuit.

For the design of the CVT ratio controller it is advantageous to reformulate to constraints in terms of clamping forces instead of pressures. Associating a clamping force $F_{\alpha,\beta}$ with the pressure $p_{\alpha,\beta}$ and using Eq. (9) and Eq. (10) this results in the requirement:

$$F_{\alpha,min} \leq F_\alpha \leq F_{\alpha,max} \qquad (18)$$

with minimum pulley clamping forces:

$$F_{\alpha,min} = \max(F_{\alpha,low}, F_{\alpha,torque}, F_{\alpha,hyd}) \qquad (19)$$

5. CONTROL DESIGN

It is assumed in this section that at each time t the primary speed $\omega_p(t)$, the ratio $r_{cvt}(t)$, and the pressures $p_p(t)$ and $p_s(t)$ are known from measurements, filtering and/or reconstruction. Furthermore, it is assumed that the CVT is mounted in a vehicular driveline and that the desired CVT ratio $r_{cvt,d}(t)$ and the desired rate of ratio change $\dot{r}_{cvt,d}(t)$ are specified by the overall hierarchical driveline controller. This implies, for instance, that at each time instant the constraint forces can be determined.

The main goal of the local CVT controller is to achieve fast and accurate tracking of the desired ratio trajectory. An important subgoal is to maximize the efficiency and to minimize belt and pulley wear. It is quite plausible (and otherwise supported by experiments, see Vroemen (2001)) that to realize this subgoal the clamping forces F_p and F_s have to be as small as possible, taking the requirements in Eq. (18) into account.

The output of the ratio controller is subject to the lower constraints in Eq. (18). The constraints $F_\alpha \geq F_{\alpha,min}$ can effectively raise the clamping force setpoint of one pulley, resulting in an undesirable ratio change. This can be counteracted by raising the opposite pulley's clamping force as well, introducing a feedforward part in the controller.

Using Ide's model, *i.e.,* using Eq. (8), expressions for the ratio change feedforward forces $F_{p,ratio}$ and $F_{s,ratio}$ can be easily derived:

$$F_{p,ratio} = F_{shift,d} + \kappa \cdot F_{s,min} \qquad (20)$$

$$F_{s,ratio} = \frac{-F_{shift,d} + F_{p,min}}{\kappa} \qquad (21)$$

where $F_{shift,d}$ is the desired shift force. As explained earlier, κ depends on τ, which in turn depends on F_s. This is an implicit relation ($F_{s,ratio}$ depends on F_s), which has been tackled by calculating κ from pressure measurements.

At each time, one of the two clamping forces is equal to $F_{\alpha,min}$, whereas the other is equal to $F_{\alpha,ratio}$ and determines the ratio. In fact, the ratio is controlled in such a way that the shifting force F_{shift} becomes equal to $F_{shift,d}$. This holds as long as the clamping forces do not saturate on their maximum constraint. In that case, the shifting speed is limited due to actuator saturation.

To complete the controller, $F_{shift,d}$ must be specified. As the dynamics of the variator (according to Ide's model) are quite nonlinear, an equivalent input u is introduced, using an inverse representation of Ide's model for $F_{shift,d}$:

$$F_{shift,d} = \frac{u + \dot{r}_{cvt,d}}{k_r \cdot |\omega_p|} \qquad (22)$$

Basically a feedback-linearizing weighting of u with the reciprocal of both $|\omega_p|$ and k_r is applied. This cancels the (known) non-linearities in the variator, see *e.g.,* Slotine and Li (1991). Further, a setpoint feedforward is introduced, which will reduce the phase lag of the controlled system responses.

Due to model inaccuracies (in the feedforwards) or due to disturbances (like the upper clamping force constraints), differences γ between $\dot{r}_{cvt}$ and $\dot{r}_{cvt,d}$ will occur:

$$\dot{r}_{cvt} = \dot{r}_{cvt,d} + u + \gamma \qquad (23)$$

Good tracking behaviour is obtained if u cancels γ well. A linear feedback controller has been chosen for u based on the knowledge that (contrary to Eq. (8)), there are inertias involved, requiring at least a 2nd order controller. Consequently, a PID controller is used. The proportional action is necessary for a rapid reduction of errors, whereas the integrating action is needed in order to track ramp ratio setpoints with zero error. Some derivative action proved necessary to gain larger stability margins (and less oscillatory responses). The controller is implemented as follows:

$$u = D \cdot \dot{r}_{\text{cvt}} +$$
$$P \cdot (r_{\text{cvt,d}} - r_{\text{cvt}}) +$$
$$I \cdot \int_0^t [k_{\text{e}} \cdot (r_{\text{cvt,d}} - r_{\text{cvt}})] \, d\tau \qquad (24)$$

where $k_{\text{e}} \in \{0,1\}$ switches the integrator on and off during actuator saturation. This is a conditional anti-windup mechanism, see *e.g.*, Bohn and Atherton (1995). The derivative action of the controller only acts on the measured CVT ratio signal to avoid an excessive controller response on stepwise changes of the ratio setpoint. Additionally, a high frequency pole has been added to the derivative operation to prevent excessive gains at high frequencies. Since the CVT is already implemented in a test vehicle, experiments on a roller bench have been performed to tune the controller parameters P, I and D manually.

6. EXPERIMENTAL RESULTS

Vehicle tests including accelerator pedal kick-downs, pedal jogging (featuring rapid accelerator pedal input changes, see Serrarens (2001)), and tip-shifting have been performed on a test track, see Fig. 5. Good ratio tracking was obtained for moderately fast and slow ratio setpoint variations. Results of an experiment with a cruise-controlled starting velocity of 50 [km/h] are depicted in Fig. 6 and Fig. 7. The CVT ratio setpoint has been generated by the coordinated controller (see Fig. 1). A new stepwise pedal input is generated every second, hence the resulting ratio setpoints changes will be very fast as well.

Fig. 5. Experimental vehicle during tests at the test track

Initially, the CVT ratio and pulley pressures are stationary and equal to their setpoints.

At t=1 [s], there is a rapid downshift. A slight "bump" in the ratio is visible at t=1.3 [s], just after the downshift has started. Here, the primary pressure peaks above its setpoint when the
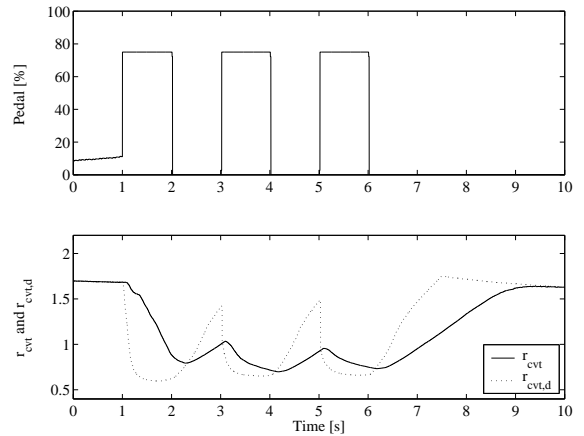

Fig. 6. CVT ratio response and tracking error, pedal jogging during road test
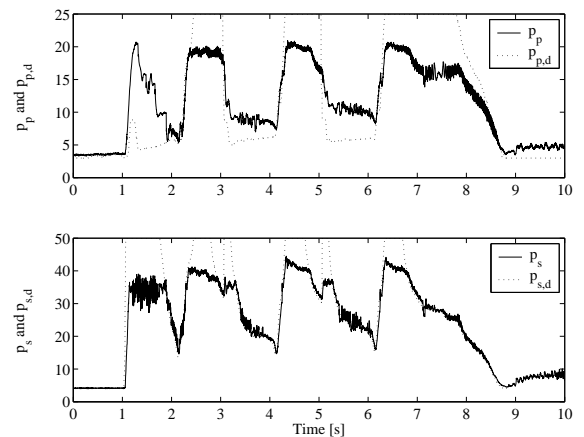

Fig. 7. Primary and secondary pulley pressures, pedal jogging during road test

secondary pressure is increased rapidly, caused by limitations in the primary pressure controller. This phenomenon also lowers the maximum downshift speed. At the start of the fast up-shifts at t=4 [s] and t=6 [s], a slight inverse response is present. Due to the layout of the hydraulic system, the secondary circuit needs to supply the primary circuit with oil. As a result, the secondary pressure rises in advance to the primary pressure and causes an initial downshift. During all of the upshifts, the ratio initially rises approximately linear. This is caused by the limited pump flow, which also causes the secondary pressure to saturate below the setpoint. Upshifting is further characterised by a slight overshoot, which is clearly visible at t=3.25 [s] and t=5.25 [s]. As the primary pressure cannot drop rapidly enough due to a limited primary valve orifice area towards the drain, upshifting continues.

The performance limitations are mainly caused by the hydraulic constraints, therefore better performance can only be obtained if the pump flow is increased (by using a larger oil pump) and the primary valve control loop is improved. An alternative hydraulic circuit is described by van

Rooij and Frank (2002), that uses two gear servo pumps in series, replacing the primary valve with a two-way pump. This practically eliminates the hydraulic constraints, imposed by the primary valve.

7. CONCLUSIONS

A new ratio controller for a metal push-belt CVT with a hydraulic belt clamping system has been developed. Based on dynamic models of the variator and hydraulics, feedforwards of system constraints, a setpoint feedforward and a linearizing feedback controller have been implemented. The feedback controller is a PID controller with conditional anti-windup protection. The total ratio controller guarantees that at least one of the pressure setpoints is always minimal with respect to its constraints, while the other is raised above the minimum level to enable shifting. This approach is beneficial with respect to efficiency and wear. Roller bench and road test experiments with a vehicle built-in CVT show that good tracking is obtained. The largest deviations from the ratio setpoint are caused by hardware limitations.

REFERENCES

Bohn, C. and D.P. Atherton (1995). An analysis package comparing PID anti-windup strategies. *IEEE Control Systems Magazine* **15**(Issue 2), 34–40.

Frank, A.A. and A. Francisco (2002). Ideal operating line CVT shifting strategy for hybrid electric vehicles. In: *Proc. of the Internat. Congress on Continuously Variable Power Transmission (CVT'02)*. VDI Berichte 1709. pp. 211–227.

Guebeli, M., J.D. Micklem and C.R. Burrows (1993). Maximum transmission efficiency of a steel belt continuously variable transmission. *Trans. of the ASME, Jrnl. of Mechanical Design* **115**, 1044–1048.

Ide, T., A. Udagawa and R. Kataoka (1994). A dynamic response analysis of a vehicle with a metal V-belt CVT. In: *Proc. of the 2nd Internat. Symp. on Advanced Vehicle Control (AVEC'94), Tsukuba, Japan*. Vol. 1.

Ide, T., A. Udagawa and R. Kataoka (1996). Experimental investigation on shift-speed characteristics of a metal V-belt CVT. In: *Proc. of the Internat. Congress on Continuously Variable Power Transmission (CVT'96)*.

Ozeki, T. and M. Umeyama (2002). Development of Toyota's transaxle for mini-van hybrid vehicles. In: *Transmission and driveline systems symposium 2002*. Vol. SP-1655.

Serrarens, A.F.A (2001). Coordinated control of the Zero Inertia powertrain. Ph.D. thesis. Technische Universiteit Eindhoven.

Shafai, E., M. Simons, U. Neff and H.P Geering (1995). Model of a continuously variable transmission. In: *Proc. of the 1st IFAC Workshop on Advances in Automotive Control*. pp. 99–107.

Slotine, J.-J. E. and W. Li (1991). *Applied nonlinear control*. Prentice-Hall.

Spijker, E. (1994). Steering and control of a CVT based hybrid transmission for a passenger car. Ph.D. thesis. Technische Universiteit Eindhoven. Eindhoven, The Netherlands.

Stouten, B. (2000). Modeling and control of a CVT. WFW-report 2000.10. Technische Universiteit Eindhoven. Eindhoven, The Netherlands.

van der Laan, M. and J. Luh (1999). Model-based variator control applied to a belt type CVT. In: *Proc. of the Internat. Congress on Continuously Variable Power Transmission (CVT'99)*. Eindhoven, The Netherlands. pp. 105–110.

van Rooij, J. and A.A. Frank (2002). Development of a 700 Nm chain-CVT. In: *Proc. of the Internat. Congress on Continuously Variable Power Transmission (CVT'02)*. VDI Berichte 1709. pp. 179–194.

Vanvuchelen, P. (1997). Virtual engineering for design and control of continuously variable transmissions. Ph.D. thesis. Katholieke Universiteit Leuven. Leuven, Belgium.

Vroemen, B.G. (2001). Component control for the Zero Inertia powertrain. Ph.D. thesis. Technische Universiteit Eindhoven. Eindhoven, The Netherlands.